Submicron thermocouple measurements of electron-beam resist heating

Dachen Chu,[a] D. Taner Bilir, and R. Fabian W. Pease
Integrated Circuits Laboratory, Stanford University, Stanford, California 94305

Kenneth E. Goodson
Mechanical Engineering Department, Stanford University, Stanford, California 94305

(Received 28 May 2002; accepted 30 September 2002)

Pattern distortion caused by resist heating is believed to contribute significantly to errors in feature size and pattern placement. A number of models have been proposed to predict the temperature rise of resist heating but experimental results are scarce. We fabricated and calibrated thin film gold/nickel thermocouples with $(400\ \text{nm})^2$ junction size and used these to measure work-piece heating during electron-beam exposure. Irradiation by a 15 kV electron beam of 600 nA and 2 μm radius caused a temperature rise of 70 K, about 15% lower than the calculated result. The discrepancy may be due to the differences between the energy deposition profiles used in modeling and those prevailing in the experiments. © *2002 American Vacuum Society.* [DOI: 10.1116/1.1523023]

I. INTRODUCTION

The continuous shrinking of transistor critical dimension (CD) keeps imposing challenges for photomask makers to meet the stringent CD tolerances.[1] Pattern distortion caused by the resist heating due to electron-beam energy deposition can be a major contributor to errors in feature size and pattern placement.[2–4] We have developed an analytical model employing multilayer Green's functions, which facilitates computation of four-dimensional temperature distributions in space and time.[5] In prior work there have been different simplifications to facilitate computation for multilayer structures. One is to neglect the resist layer and assume that the resist temperature is the same as the surface temperature of substrate;[6–8] another is to assume that the substrate is an ideal heat sink.[9] Those different assumptions lead to very different results. The maximum temperature increase was calculated to be 14 K in Ref. 7 and 750 K in Ref. 9. Some authors published temperature distributions for multilayer structures without describing their mathematical treatment in detail.[10,11] A detailed solution of our model using the multilayer Green's functions was described in Ref. 5. We found that the formulas used in Refs. 6, 7, and 9 dealt with the specific cases of our general solution.

However, temperature measurements to verify the resist heating calculations are needed. Babin *et al.* measured the *in situ* temperature rise using a $YBa_2Cu_3O_7$ superconducting thermometer with 3 μm spatial resolution. But, the experiment was conducted at a liquid nitrogen temperature[12] and it does not resemble the normal thermal environment of electron-beam writing. Iranmanesh and Pease reported silicon surface temperature measurement under electron-beam irradiation with a thin film thermocouple (TFTC),[13] but the spatial resolution was also larger than 2 μm. Since the spatial resolution is a key factor in the highly localized resist heating measurement, TFTC is a good candidate because high spatial resolution can be achieved by minimizing its junction size. A small sensing volume can also produce a faster response time[14,15] and a minimum distortion to the temperature field. The values of the Seebeck coefficients of the materials in a TFTC can be different from those of the same materials in bulk form, so calibration is important.

We have made gold/nickel thermocouples with $(400\ \text{nm})^2$ junction size and have used them to measure temperature profiles at the bottom surface of resist during electron-beam exposure. The peak temperature rise measured was 15% lower than the calculated value. This may be due to the differences between the energy deposition profiles used in modeling and those prevailing in experiments.

II. EXPERIMENTAL PROCEDURE

A. Fabrication of TFTCs

Nickel and gold were chosen to be the two components of the TFTC because of their large difference in Seebeck coefficient, and their robustness in processing. The TFTC (Fig. 1) was fabricated on 1 μm SiO_2 on silicon. Electron-beam lithography and liftoff were used to pattern the TFTC. Electron-beam resist ZEP520 was used because its undercut profile facilitates liftoff. The nickel and gold were evaporated at a pressure of 10^{-6} Torr. The nickel layer (100 nm thick) was deposited first. The gold layer (200 nm thick) was also used to define the contact pads for wire bonding. After the TFTC was fabricated, a 300 nm layer of poly(methylmethacrylate) (PMMA) was coated on top of the wafer for subsequent resist heating measurements. The PMMA layer also functioned as a protection layer for the TFTC.

B. Calibration of TFTC

Since our motivation is to measure the temperature difference between the highly local electron beam heated region and the unheated region on a wafer, both the measurement and reference junctions are on the wafer. Also as the TFTC is used to measure the temperature difference between different locations on a wafer, a local heating source is needed close to the calibration structure. As shown in Fig. 2, a metal line 10 μm wide was patterned in a serpentine manner with a number of identical folds for calibration. The metal line functions as a local joule-heating source so that within each fold the

[a]Electronic mail: dcchu@standford.edu

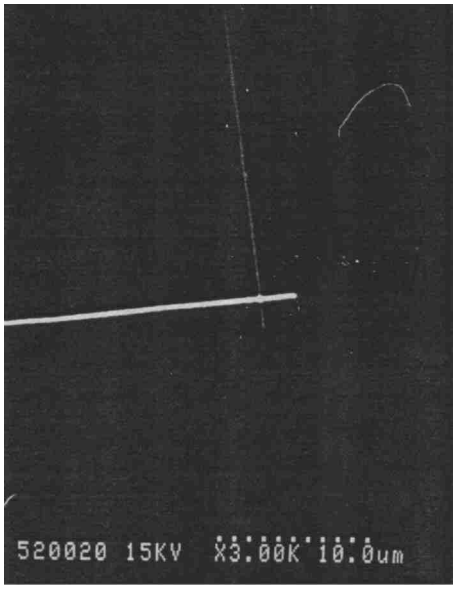

FIG. 1. SEM picture of a typical gold/nickel TFTC with 400 nm junction size.

temperature distributions are the same. A resistive thermometer is patterned in one fold and the TFTCs were patterned inside the other. To eliminate the possible error generated by the nonuniformity of local temperature field, both the resistive thermometer and the TFTCs were patterned at similar locations inside the folds.

First, the resistive thermometer (made of gold) is self-calibrated in a cryostat. The four-probe resistance measurements determine the room temperature resistance of 1.5 Ω and a resistive temperature sensitivity of 0.004 Ω/K. Then the TFTC is calibrated against the resistive thermometer when heated by the 10 μm gold metal line. The result of calibration is shown in Fig. 3.

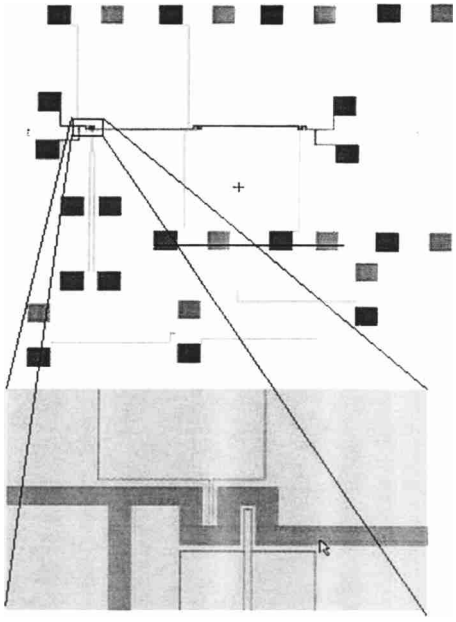

FIG. 2. Top view of a mask layout of TFTCs with calibration structure. In the middle of the picture a 10 μm wide metal line was patterned with a number of folds for calibration. The magnified part is zoomed on the two folds. The TFTC patterned inside the left fold is calibrated by the resistive thermometer patterned inside the right fold.

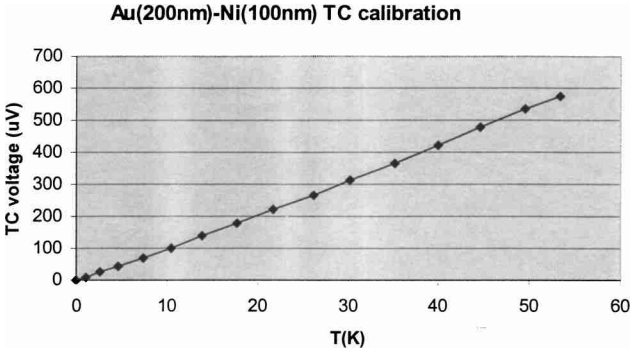

FIG. 3. Calibration result shows that the Seebeck coefficient of the gold/nickel TFTC is 10 μV/K.

The calibrated Seebeck coefficient of the Au(200 nm)/Ni(100 nm) TFTC is 10.1 μV/K, about half of the bulk value.[16]

C. Temperature measurements

The *in situ* temperature measurements were carried out in a modified Hitachi S2500 scanning electron microscope (SEM). The differential signal was monitored on a digital oscilloscope (Tektronix™ TDS 460 A) after amplification by a voltage amplifier (SRS™ SR570) (Fig. 4). Inside the SEM the electron beam was slowly (20 μm/s) scanned across the thermocouple junction, and the output of the TFTC was recorded. Based on diffusion theory, the time for heat to diffuse through the 1 μm thick oxide can be estimated to be $T=(1\ \mu\text{m})^2/\alpha \approx 1.2\ \mu$s. Where the thermal diffusivity of

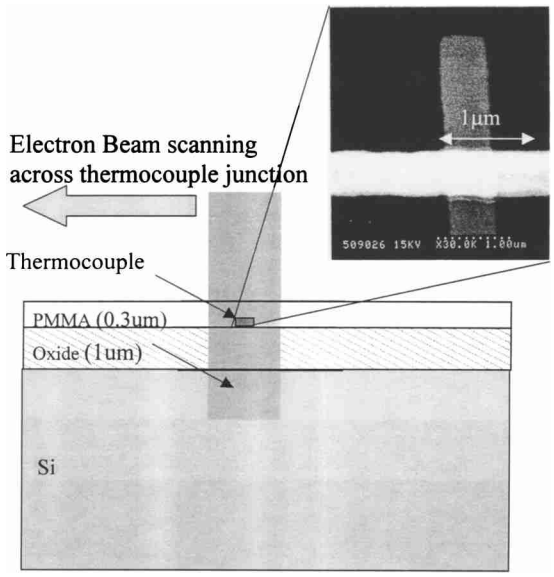

FIG. 4. Experimental diagram. As an electron beam scans across the TFTC junction, the temperature profile at the bottom side of the resist is measured by the TFTC. The SEM picture shows the magnified TFTC junction.

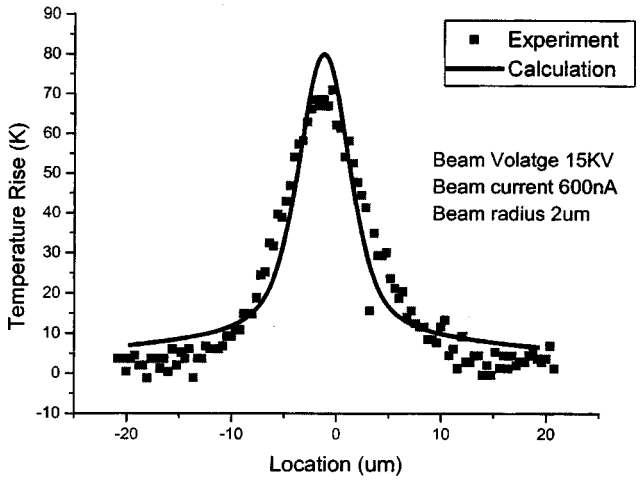

FIG. 5. Experimental and calculated temperature profile at the bottom surface of resist, irradiated by a 15 kV Gaussian beam. Beam current i_b is 600 nA and beam radius r_b is 2 μm.

oxide is $\alpha = 0.84\ \mu m^2/\mu s$. Similarly the time for heat to diffuse through 0.3 μm thick resist is also about 1 μs. The diffusivity of the silicon substrate is 2 orders magnitude higher than that of the oxide, therefore the heat diffusion time in silicon substrate is negligible. Since the scan time is much longer than the heat diffusion time, the measured temperature profile is virtually steady state. We carefully checked to make sure the source of the signal was not due to scattering electrons. On the same chip we fabricated a ''dummy'' thermocouple junction consisting of a single material, which is meant to yield zero thermal signal. When the beam was scanned across the dummy junctions, no appreciable signal was detected. Similarly no signal was observed when the beam was scanned across the TFTC far away from the junction.

Experiments were carried out with different thermocouples and under different conditions. One representative result is shown in Fig. 5 along with the simulation results from the multilayer Green's function model. The electron beam was assumed to take a Gaussian shape:

$$j(r) = \frac{i_b}{2\pi r_b^2} \exp\left(\frac{-r^2}{2r_b^2}\right),$$

where i_b represents the beam current and r_b represents the beam radius where the current density j drop to 60.9% of its maximum value. Experimentally we measured i_b and r_b to be 600 nA and 2 μm, respectively.

The simulation results are systematically sharper than the experimental results. The discrepancy may arise from the following factors. (a) The lateral energy spread in Monte Carlo simulation may be underestimated. (b) The beam radius was measured by scanning the e beam over a knife-edge structure. The measurement uncertainty in radius was estimated to be about 10%. Simulation results showed that an increase of beam size by 10% would reduce the discrepancy. (c) The actual beam shape may deviate from a perfect Gaussian curve. (d) The measured temperature is an average value over the TFTC junction. The finite junction size may lose some temperature gradient information and yield a flatter profile than the actual temperature profile. Further shrinking the junction size would reduce this error but the physics of TFTC junctions exposed to a nonequilibrium temperature field is worth exploring. (e) In the Green's function model the surface radiation and thermal conduction through the arms of the TFTC are neglected. However, the overestimation in temperature caused by this assumption is not significant because the thermal resistance due to radiation and conduction through these arms is more than 1 order of magnitude larger than the thermal resistance due to substrate conduction. (f) Finally the thermal effect of the chemical reaction induced by electron exposure of the resist was neglected.

III. SUMMARY AND CONCLUSIONS

Gold/nickel thin film thermocouples with 400 nm spatial resolution have been fabricated, calibrated, and used to measure the temperature profile at the bottom surface of a resist film during electron-beam exposure. A steady-state temperature rise of 70 K was observed under the irradiation of a Gaussian shaped e beam of 15 kV voltage, 600 nA beam current, and 2 μm beam radius. This temperature rise can cause a change of 36% in PMMA sensitivity.[17] Calculated peak temperatures are about 15% higher than the measurements but this discrepancy is not significant. Transient measurements are planned; the expected temporal resolution is on the order of 1 μs.

ACKNOWLEDGMENTS

This work is supported by Intel and SRC via Contract No. MJ-653. The authors acknowledge Min Bai for her Monte Carlo simulation work of energy deposition profile, James Conway for his technical support in e-beam systems, and Fu-Chang Lo and the Mask Advisory Group for their useful discussions.

[1]SIA Roadmap http://public.itrs.net/files/1999_SIA_Roadmap/Home.htm
[2]E. Kratschmer and T. Groves, J. Vac. Sci. Technol. B **8**, 1898 (1990).
[3]M. Yasuda, H. Kawata, K. Murata, K. Hashimoto, Y. Hirai, and N. Nomura, J. Vac. Sci. Technol. B **12**, 1362 (1994).
[4]S. Babin, J. Vac. Sci. Technol. B **15**, 2209 (1997).
[5]D. Chu, R. F. W. Pease, and K. Goodson, Proc. SPIE **4689**, 206 (2002).
[6]A. Iranmanesh and R. F. W. Pease, J. Vac. Sci. Technol. B **1**, 91 (1983).
[7]H. Ralph *et al.*, Proceedings of the 10th International Conference on Electron and Ion Beam Science and Technology.
[8]T. R. Groves, J. Vac. Sci. Technol. B **14**, 3839 (1996).
[9]T. Abe, K. Ohta, H. Wada, and T. Takigawa, J. Vac. Sci. Technol. B **6**, 853 (1988).
[10]E. V. Drift, A. C. Enters, and S. Radelaar, J. Vac. Sci. Technol. B **9**, 3470 (1991).
[11]S. Babin, I. Y. Kuzmin, and G. Sergeev, Proc. SPIE **2884**, 520 (1996).
[12]S. Babin, M. E. Gaevski, and S. G. Konnikov, J. Vac. Sci. Technol. B **19**, 153 (2001).
[13]A. Iranmanesh and R. F. W. Pease, J. Vac. Sci. Technol. B **1**, 739 (1983).
[14]D. Burgess, M. Yust, and K. G. Kreider, Sens. Actuators A **24**, 156 (1990).
[15]A simple *RC* model predicts the time response of our 400 nm sensor is on the order of 10 ns.
[16]*Thermal Sensors*, edited by G. C. M. Meijer and A. W. Herwaarden (Institute of Physics, Bristol, 1994), p. 107.
[17]S. Babin, P. Hudek, and I. Kostic, J. Vac. Sci. Technol. B **15**, 311 (1997).